16. (a) N. Gō and H. A. Scheraga, *J. Chem. Phys.*, **51**, 4751 (1969); (b) *Macromolecules*, **9**, 535 (1976).
17. M. Karplus and J. N. Kushick, *Macromolecules*, **14**, 325 (1981).
18. Y. K. Kang and M. S. Jhon, *Macromolecules*, **17**, 138 (1984).
19. (a) Y. K. Kang and D. W. Kim, *Bull. Korean Chem. Soc.*, **11**, 144 (1990); (b) Y. A Shin and Y. K. Kang, *ibid.*, **12**, 61 (1991); (c) Y. K. Kang, *Int. J. Pept. Protein Res.*, **38**, 79 (1991).
20. (a) R. M. Levy, O. Rojas, and R. A. Freisner, *J. Phys. Chem.*, **88**, 4233 (1984); (b) J. Brady and M. Karplus, *J. Am. Chem. Soc.*, **107**, 6103 (1985).
21. G. Ravishanker, M. Mezei, and D. L. Beveridge, *J. Comput. Chem.*, **7**, 345 (1986).
22. (a) IUPAC-IUB Commission on Biochemical Nomenclature, *Biochemistry*, **9**, 3471 (1970); (b) IUPAC-IUB Joint Commission on Biochemical Nomenclature, *J. Biol. Chem.*, **260**, 14 (1985).
23. S. S. Zimmerman, M. S. Pottle, G. Némethy, and H. A. Scheraga, *Macromolecules*, **10**, 1 (1977).
24. The letter codes of C, E, A, F, and A* denote the C_7^{eq}, the extended (*e.g.* C_5), the right-handed α-helical (α_R), the proline type II (p_{II}), and the left-handed α-helical (α_L) conformations; other letter codes of D and G represent the remaining conformations to indicate contiguity (see ref. 23 for detaills).
25. (a) G. Némethy, M. S. Pottle, and H. A. Scheraga, *J. Phys. Chem.*, **87**, 1883 (1983); (b) M. J. Sippl, G. Némethy, and H. A. Scheraga, *ibid.*, **88**, 6231 (1984).
26. D. M. Gay, *ACM Trans. Math. Software*, **9**, 503 (1983).
27. M. Vásquez, G. Némethy, and H. A. Scheraga, *Macromolecules*, **16**, 1043 (1983).
28. In ref. 27, the energy was minimized with respect to backbone and side chain dihedral angles only, where the dihedral angles of peptide bonds and end groups were held fixed at 180°.
29. In this work, seven low-energy conformations with relative conformational energy $\Delta E<3.0$ kcal/mol in ref. 27 were used as starting conformations because two remaining conformations show relatively high energy states, *i.e.*, $\Delta E>5.0$ kcal/mol.
30. R. C. Weast, ed., *CRC Handbook of Chemistry and Physics*, 66th ed., CRC, Boca Raton, 1985.
31. (a) M. Mezei, P. K. Mehrotra, and D. L. Beveridge, *J. Am. Chem. Soc.*, **107**, 2239 (1985); (b) P. K. Mehrotra and D. L. Beveridge, *ibid.*, **102**, 4287 (1980).
32. In ref. 8b, we optimized the hydration shell radius of ether oxygen to be bigger than the location of the first minimum in the O···O rdfs of the Monte Carlo simulation of methanol in water because use of the latter value gives poor agreement for the hydration free energies of ethers. The optimized value was used in determining the hydration shell radii of other polar atoms. So the large coordination numbers may be caused by these large values of the hydration shell radii.
33. V. Madison and K. D., Kopple, *J. Am. Chem. Soc.*, **102**, 4855 (1980).

EPR Study of the High T_c Superconductor $YBa_2Cu_3O_{7-y}$ Doped with Palladium or Zinc

Hag Chun Kim, Hyunsoo So*, and Ho Keun Lee†

Department of Chemistry, Sogang University, Seoul 121-742
†Korean Standards Research Institute, Taejeon 302-340. *Received April 15, 1991*

EPR spectra of the high T_c superconductor $YBa_2Cu_3O_{7-y}$ (YBCO) doped with Pd^{2+} or Zn^{2+} have been measured at several temperatures and dopant concentrations. The spectral intensity of $YBa_2(Cu_{1-x}Pd_x)_3O_{7-y}$ is proportional to the dopant concentration. The behavior of $YBa_2(Cu_{1-x}Zn_x)_3O_{7-y}$ is quite different: the spectral intensity remains almost constant up to $x=0.10$ and then increases rapidly above $x=0.10$. The results are interpreted in terms of localized and antiferromagnetically spin-paired *d* holes in both CuO chain and planes. The Pd^{2+} ion substitutes on the CuO chain consisting of "CuOCu dimers", and a Cu^{2+} ion with an unpaired spin is generated for each Pd^{2+} ion substituted. On the other hand, Zn^{2+} substitutes on the CuO planes, and all or most of the spins in the two-dimensional plane manage to pair up in the region of low dopant concentration. When the dopant concentration exceeds a certain limit, it becomes more difficult for the spins to find partners, and the number of unpaired spins increases rapidly with increasing dopant concentration. The Zn^{2+} ion is more effective than the Pd^{2+} ion in suppressing the superconductivity of YBCO. This is attributed to the fact that Zn^{2+} substitutes on the CuO planes which are mainly responsible for the superconductivity, while Pd^{2+} substitutes on the CuO chain which is of secondary importance in the superconductivity.

Introduction

Various experimental techniques have been used to study the high T_c superconductor $YBa_2Cu_3O_{7-y}$ (YBCO) first prepared by Wu *et al.*[1] We are using electron paramagnetic resonance (EPR) spectroscopy to study high T_c superconductors.

Since EPR can give information on the unparied electrons in the system, it might be useful in clarifying the nature of the superconducting mechanism.

Previously we studied the EPR spectra[2] of pure YBCO and also YBCO doped with Yb^{3+} or Gd^{3+}. Samples of pure YBCO exhibit a weak EPR signal which accounts for less than 1% of the copper ions in the compound. This indicates that most Cu^{2+} ($3d^9$) ions in the sample are EPR inactive. Then the weak EPR signal should be attributed to either paramagnetic defects in YBCO or to impurity phases in the sample. Any paramagnetic defect in the superconductor may be useful as a spin probe for studying the electronic structure of the superconductor and the superconducting mechanism. The paramagnetic ion in the impurity phase cannot be used as a spin probe.

We have shown that Yb^{3+} ($4f^{13}$) or Gd^{3+} ($4f^7$), which replaces Y^{3+} in YBCO, exhibits good EPR spectrum.[2] But these ions, located quite far away from the CuO planes, are not very sensitive as spin probes for the superconductivity.

In this study we have used diamagnetic dopants Pd^{2+} and Zn^{2+} in order to create paramagnetic centers in YBCO. (The doped compounds are designated as Pd/YBCO and Zn/YBCO below.) A diamagnetic dopant in a Cu^{2+} site is expected to prevent some Cu^{2+} ions from forming spin pairs. There are two kinds of copper sites in YBCO : Cu(1) in the CuO chain having a square planar environment and Cu(2) in the CuO planes having a square pyramidal environment. It is known that Pd^{2+} substitutes at the Cu(1) site exclusively.[6] A neutron diffraction study has shown that Zn^{2+} substitutes at the Cu (2) site exclusively,[4] but another similar study finds Zn^{2+} substitutes at both Cu(2) and Cu(1) sites.[5] Since the Zn^{2+} ion is rarely found in a square planar environment, it is more likely that Zn^{2+} substitutes at the Cu(2) site. Therefore, studies on YBCO doped with Pd^{2+} and Zn^{2+} provide an opportunity to compare the effect of doping preferentially one of the two copper sites.

The electrical resistivity of $YBa_2(Cu_{1-x}Pd_x)_3O_{7-y}$ with $x=0.1$ was reported before.[6] And while we were working on Zn/YBCO, some studies on the same system were reported by others.[7]

Experimental

Preparation of Compounds. YBCO doped with Pd^{2+} was prepared by three different methods.

Method 1. This is the method used by Ferey *et al.*[6] $BaCO_3$, BaO_2, CuO, Y_2O_3, and Pd were mixed according to the formula $YBa_2(Cu_{1-x}Pd_x)_3O_{7-y}$ ($x=0$-0.15) and pulverized. The mixture was calcined at 820℃ for 20 hours. When the calcined, black sample contained green component, calcination was repeated. During calcination BaO_2 is decomposed into BaO and O_2, and Pd is oxidized to Pd^{2+} by O_2. After calcination the sample was pulverized again and pressed into pellets of 10 mm in diameter. These pellets were sintered under flowing oxygen at 820℃ for 20 hours, annealed at 500 ℃ for 5 hours, and cooled slowly to room temperature.

Method 2. $BaCO_3$, CuO, Y_2O_3, and PdO were mixed according to the appropriate composition, and calcined at 820℃ for 22 hours. After that the same procedure as in Method 1 was followed.

Method 3. $BaCO_3$, CuO, Y_2O_3, and PdO were mixed according to the appropriate composition, and dissolved in nitric acid. Citric acid was added to the solution, and then the resulting precipitate was treated with ethylene glycol. The mixture was heated, and the resulting polymer containing metal ions was calcined at 700-800℃ for 20 hours. After calcination the sample was treated by the same procedures as in Method 1.

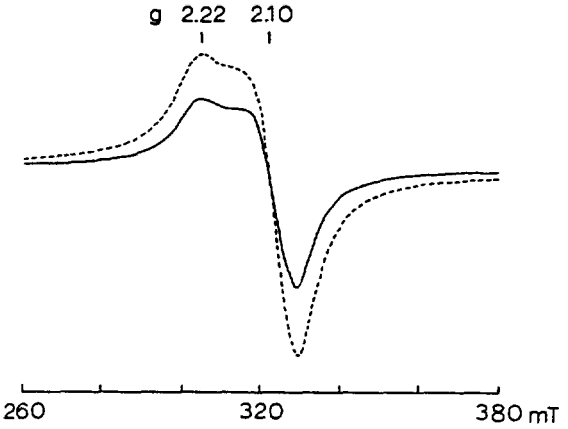

Figure 1. EPR spectra of $YBa_2(Cu_{1-x}Pd_x)_3O_{7-y}$ ($x=0.02$) at 250 K (——) and 95 K (----).

YBCO doped with Zn^{2+} was prepared in the following way. Powders of $BaCO_3$, Y_2O_3, CuO, and ZnO were mixed according to the formula $YBa_2(Cu_{1-x}Zn_x)_3O_{7-y}$ ($x=0$-0.17), and calcined at 950℃ for 24 hours. The mixture was pressed into pellets, and the pellets were sintered under flowing oxygen at 950℃ for 12 hours. Then the pellets were annealed under flowing oxygen at 500℃ for 18 hours, and cooled slowly to room temperature.

Measurements. DC electrical resistance was measured using the standard four-probe method. The measurements were made by reading the voltage drop across the inner leads of the sample while maintaining a constant sample current of less than 1.0 mA. Samples were attached to the cold finger of a closed cycle refrigerator (Palm Beach Cryophysics Model 4075) and the electrical resistance was measured as a function of temperature.

EPR spectra at 95-300 K were recorded on a Bruker EPR spectrometer (Model ER 200E) equipped with a variable temperature accessory. The spectrum at 77 K was recorded using a liquid nitrogen Dewar vessel. $CuSO_4 \cdot 5H_2O$ was used as an external reference to determine the absolute intensity of the spectrum. The intensity was determined by numerical double integration of the first derivative curve.

Results and Discussion

Pd/YBCO

Since the melting point of PdO is 870℃, samples of $YBa_2(Cu_{1-x}Pd_x)_3O_{7-y}$ ($x=0.01$-0.15) with different x values were prepared below this temperature. Samples prepared at 900℃ showed the same EPR spectra as the pure YBCO, indicating that Pd^{2+} had not replaced Cu^{2+} in YBCO. The EPR spectra for two samples with $x=0.02$ and 0.15 will be described in detail below.

$YBa_2(Cu_{1-x}Pd_x)_3O_{7-y}$ ($x=0.02$). The EPR spectrum for the sample with $x=0.02$ is shown in Figure 1. The spectrum is similar to that of Y_2BaCuO_5 (this is an impurity phase

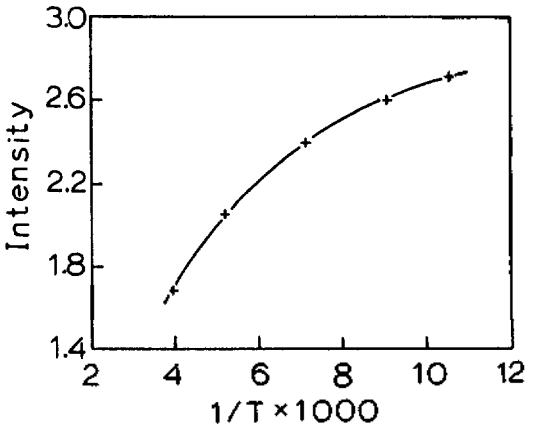

Figure 2. Temperature dependence of EPR intensity for $YBa_2(Cu_{1-x}Pd_x)_3O_{7-y}$ ($x=0.02$). Intensity is in an arbitrary unit.

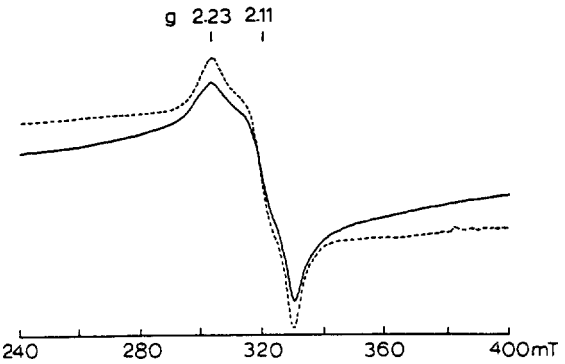

Figure 3. EPR spectra of $YBa_2(Cu_{1-x}Pd_x)_3O_{7-y}$ ($x=0.15$) at 300 K (——) and 77 K (-----).

called the green phase[8,9]), the tetragonal phase of YBCO[2], or YBCO doped with zinc[7a]. Therefore the spectrum can be ascribed either to the Cu^{2+} ions in an impurity phase or to paramagnetic Cu^{2-} ions generated by doping with Pd^{2+} ions.

Samples of YBCO often contain some impurity phases such as Y_2BaCuO_5 and $BaCuO_2$,[11] which can be reduced to less than 1% of the total copper atoms in YBCO by careful preparation.[2] Our samples, having been prepared below 850°C, may contain a samll amount of these impurities. However, the temperature dependence of the spectral intensity is quite different from that of an impurity phase. The intensity of the spectrum originating in localized unpaired electrons increases as the temperature is lowered, and it is linear with respect to $1/T$.[10] The spectrum of Y_2BaCuO_5 or $BaCuO_2$ behaves in this way,[8,9,11] while the temperature dependence of the spectrum for Pd/YBCO deviates significantly from the linearity as shown in Figure 2.

Moreover, the spectral intensity increases with increasing x (see below), indicating that unpaired spins generated by doping with Pd^{2+} contribute to the spectrum. If it is assumed that one Cu^{2+} ion with an unpaired spin is generated for each Pd^{2+} ion substituted, the number of unpaired electrons will be equal to that of Pd^{2+} ions; see below.

$YBa_2(Cu_{1-x}Pd_x)_3O_{7-y}$ ($x=0.15$). The EPR spectrum for the sample with $x=0.15$ is shown in Figure 3. The spectrum is similar to that of $YBa_2(Cu_{1-x}Pd_x)_3O_{7-y}$ ($x=0.02$), except that it has broad wings. The low temperature spectrum has even broader wings.

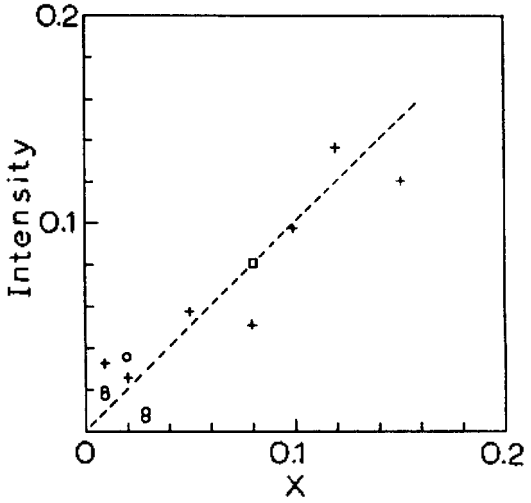

Figure 4. EPR intensity of $YBa_2(Cu_{1-x}Pd_x)_3O_{7-y}$ as a function of the dopant concentration. Samples prepared by Methods 1, 2 and 3, are designated by ○, +, □, respectively. The dashed line represents the intensity expected when one Cu^{2+} ion with unpaired spin is generated for each Pd^{2+} ion substituted.

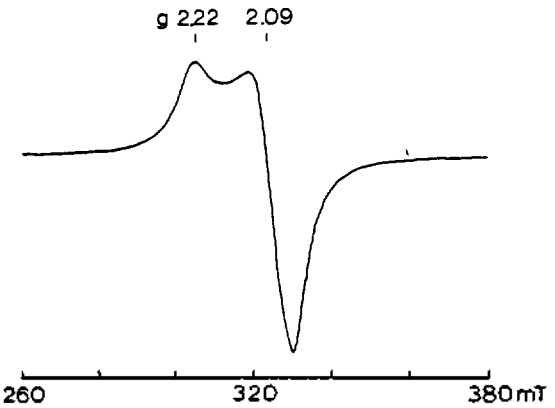

Figure 5. EPR spectrum of $YBa_2(Cu_{1-x}Zn_x)_3O_{7-y}$ ($x=0.14$) at 296 K.

The broad wings may be attributed to the magnetic dipolar interaction which becomes more important as the concentration of Pd^{2+} increases. If Pd^{2+} replaces only Cu(1) in the CuO chain,[3] the composition corresponding to $x=0.15$ is $YBa_2Cu(2)_2Cu(1)_{0.55}Pd_{0.45}O_{7-y}$. This means that 45% of the Cu(1) site is occupied by Pd^{2+}. Therefore, a large fraction of the CuO chain has the configuration -Cu-O-Pd-O-Cu-O-Pd-, and the dipolar interaction between the Cu^{2+} ions separated by an O-Pd-O group is expected to broaden the spectrum.[28]

Dependence on Dopant Concentration. The absolute intensity of the spectrum is plotted as a function of the concentration of Pd^{2+} in Figure 4. Although the points are scattered, it is seen that the intensity is roughly proportional to the concentration of Pd^{2+}. The dashed line in the figure represents the intensity expected when the number of Cu^{2+} ions contributing to the spectrum is equal to that of Pd^{2+} ions substituted. The measured intensity agrees roughly with this line, suggesting that one Cu^{2+} ion with unpai-

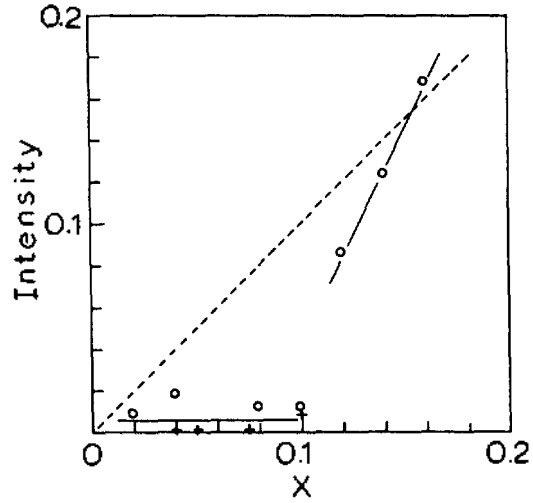

Figure 6. EPR intensity of $YBa_2(Cu_{1-x}Zn_x)_3O_{7-y}$ as a function of the dopant concentration. The data designated by ○ are taken from ref. 7(a). The dashed line represents the intensity expected when one Cu^{2+} ion with unpaired spin is generated for each Zn^{2+} ion substituted.

red spin is produced for every Pd^{2+} ion.

Zn/YBCO

A typical EPR spectrum of YBCO doped with Zn^{2+} is shown in Figure 5. This spectrum is again very similar to that of the green phase or Pd/YBCO. Thus the spectrum may be attributed to the Cu^{2+} ions in the compound.

While we were working on this system, Jee *et al.* reported an extensive study on the same system.[7a] Our EPR work agrees with their measurements. The dependence of spectral intensity on the concentration of Zn^{2+} is shown in Figure 6. The dashed line in the figure represents the intensity expected when one Cu^{2+} ion with unpaired spin is formed by each Zn^{2+} ion substituted. It is clearly seen that the measured intensity does not follow this line: it is almost independent of concentration below $x=0.10$. This suggests that unpaired spins localized on Cu^{2+} ion are not generated when a small portion of Cu^{2+} ions in the CuO plane is replaced by Zn^{2+}. Above $x=0.10$ the spectral intensity increases more rapidly than the dashed line, indicating that unpaired spins localized on Cu^{2+} ions are produced. (The slope of the solid line is about twice that of the dashed line.)

Electronic Structure of YBCO

Copper ions in both CuO chain and CuO planes have an average oxidation state of +2. Each Cu^{2+} ($3d^9$) ion can have a localized 3*d* electron hole or contribute one to a conduction band (These holes are designated as *d* holes below). In addition, $YBa_2Cu_3O_{7-y}$ has (1-2*y*) electron holes (*p* holes) in *p* orbitals of oxygen atoms.

However, there is no consensus about whether these electron holes are localized or delocalized. YBCO is metallic above T_c, and measurements of the normal state magnetic susceptibility have revealed that it has weak Pauli paramagnetism,[12] indicating that there are mobile electron holes.[13] Some authors believe that all electron holes are mobile, while others think only some specific holes are mobile.

The NMR relaxation studies provide important clues to this problem. The nuclear spin-lattice relaxation rate on the oxygen sites in the CuO planes is consistent with the metallic Korringa law,[14] indicating that the *p* holes in the CuO planes are mobile. On the other hand, the nuclear relaxation rates on Cu(1) and Cu(2) sites are non-Korringa-like, and their behaviors have been interpreted on the basis of localized *d* holes.[15-17] No direct NMR data are available for the oxygen atoms in the CuO chain. By comparing the total number of *p* holes with the electrical conductivity for a series of YBCO doped with various elements, it has been shown that the *p* holes in the CuO chain are localized while those in the CuO planes are mobile.[18] So we will assume that only *p* holes in the CuO planes are mobile, all others being localized on Cu^{2+} ions or O^{2-} ions.

YBCO is EPR-silent, and any model of its electronic structure should be able to explain this. If the unpaired electrons are mobile, the EPR-silence can be attributed to short relaxation time.[19] If the unpaired electrons are localized, they must be antiferromagnetically spin-coupled with adjacent electrons. $YBa_2Cu_3O_{7-y}$ ($y=0.1$, YBCO) is not an antiferromagnet,[20] but $YBa_2Cu_3O_{7-y}$ ($y=1$) is an antiferromagnet insulator. When *y* decreases (*i.e.*, the number of oxygen atom increases), it changes to a metallic state and the long-range antiferromagnetic order is destroyed. But if the *d* holes remain localized on Cu^{2+} ions even in the metallic state, it is quite probable that local antiferromagnetic coupling is maintained.

Now we discuss our results in terms of the above model. It has been shown that Pd^{2+} substitutes exclusively at the Cu(1) site in the CuO chain.[3] The EPR intensity of Pd/YBCO, which is proportional to the dopant concentration, indicates that the unpaired spins generated by doping with Pd^{2+} are localized on Cu^{2+} ions. If they were delocalized, they would not contribute to the EPR spectrum because of short relaxation time. The EPR spectrum of Pd/YBCO is also consistent with localized *d* holes in the CuO chain. If they were delocalized, even localized spins generated by doping with Pd^{2+} ions would exhibit a very broad EPR spectrum, much broader than the measured one, because of the magnetic interaction between the localized spins and the mobile electrons.[21,22]

However, the temperature dependence of the EPR intensity (Figure 2) suggests that these localized spins pair up partially at low temperature. Since the *d* holes with unpaired spins are separated by at least one -O-Pd-O- group in the one-dimensional chain, spin-pairing between two *d* holes is not likely to occur even at low temperatures. It is plausible that *p* holes pair up with *d* holes to reduce the number of unpaired spins at low temperatures. More work is needed to understand the temperature dependence of the EPR intensity for Pd/YBCO.

There have been two conflicting reports about the site at which the Zn^{2+} ion substitutes.[4,5] As mentioned in the Introduction section, we believe that Zn^{2+} substitutes at the Cu(2) site exclusively. If it also substitutes at the Cu(1) site,[5] the intensity of the EPR spectrum should increase significantly with increasing dopant concentration. But this has not been observed for Zn/YBCO for the region of small dopant concentration.

If the *d* holes in the CuO planes are mobile, the behavior of the EPR intensity of Zn/YBCO can be explained by assuming that no localized unpaired spins are generated by doping with Zn^{2+} ions. Since we assume that the *d* holes in the

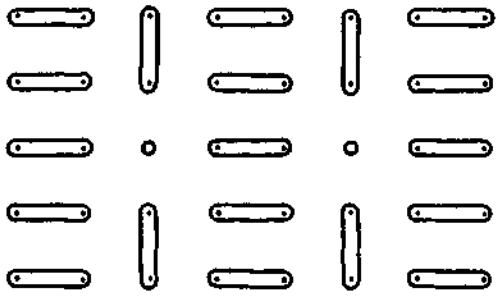

Figure 7. A possible spin pairing in a two-dimensional plane having dopant atoms representes by ○.

CuO planes are localized and spin-paired, a different mechanism is needed to explain the intensity of the EPR spectrum. When each *d* hole in one-dimensional CuO chain is spin-paired with an adjacent *d* hole, we may visualize the chain as consisting of "CuOCu dimers". Then one unpaired spin must be generated for each Pd^{2+} ion substituted in the CuO chain. But the situation is different for the two-dimensional CuO plane, where each Cu^{2+} ion has four neighboring Cu^{2+} ions. If antiferromagnetic spin-pairing stabilizes the system, then all or most of the spins can still form pairs, when the dopant concentration is not very large; see the example in Figure 7. When the dopant concentration is large, the number of spins which cannot find partners will increase.

This electronic structure is closely related with resonating valence bond (RVB) model. It has been shown that the one-dimensional Heisenberg antiferromagnetic chain is not of the Néel type.[23] For this reason, Anderson proposed that in certain situations the ground state is closer to one in which pairs of spins are bound into singlet states.[24] Since in general the spins can be paired in several alternative ways, the actual ground state is a superposition over such products of singlets. For one-dimensional chain there are only two resonance structures, and the probability of resonance is very small. So its ground state may consist pairs of spins. For two-dimensional plane there can be several resonance structures. However, any defect such as *p* holes in the plane and dopant atoms will reduce the number or resonance structures. So the ground state of the doped plane may also be close to one consisting of CuOCu dimers.

Effect of Dopants on Superconductivity

T_c of Pd/YBCO is found to decrease slowly with increasing dopant concentration. So $YBa_2(Cu_{1-x}Pd_x)_3O_{7-y}$ with $x=0.17$ is still a superconductor with $T_c=47$ K.[6] In the early stage of research on YBCO it was not clear whether the CuO plane or the CuO chain is responsible for the superconductivity. But now it is generally accepted that the CuO plane is more important than the CuO chain. Actually, such high T_c superconductors as Bi-Sr-Ca-Cu-O and Tl-Ba-Ca-Cu-O have only CuO planes.[29,30] This explains why T_c decreases slowly with increasing dopant concentration for Pd/YBCO which has dopants in the CuO chain.

Zn^{2+} substituted at YBCO is more effective than Pd^{2+} in suppressing the superconductivity. T_c of $YBa_2(Cu_{1-x}Zn_x)_3O_{7-y}$ decreases rapidly with increasing dopant concentration, and the compound ceases to be a superconductor at $x=0.10$. This is expected, for Zn^{2+} substitutes at the CuO planes which are responsible for the superconductivity. It has been argued that Zn^{2+} ($3d^{10}$) suppresses superconductivity effectively because it has no *d* hole.[25] However, the Ni^{2+} ion, which has an electronic configuration of $3d^8$ (similar to that of Pd^{2+}) and substitutes nearly uniformly at both Cu(1) and Cu(2) sites, is as effective as Zn^{2+} in suppressing the superconductivity of YBCO.[26] Similarly three dopants for $La_{1.85}Sr_{0.15}Cu_{1-x}M_xO_y$ (M=Zn, Ni, or Co) have been found to have a similar effect on T_c.[27] This suggests that dopants in the CuO planes in general lead to an effective destruction of the long-range superconducting order.

In summary, the EPR intensity of Pd/YBCO is proportional to the dopant concentration. This is attributed to generation of one Cu^{2+} ion having unpaired spin for each Pd^{2+} ion substituted in the CuO chain. The EPR intensity of $YBa_2(Cu_{1-x}Zn_x)_3O_{7-y}$ is nealy independent of the dopant concentration for $x<0.1$. This can be interpreted in terms of flexible spin pairing in the two-dimensional CuO plane at which Zn^{2+} substitutes. By comparing several dopants (Pd^{2+}, Zn^{2+}, and Ni^{2+}), we have found that the substitutional site is the most important factor affecting the superconductivity.

Acknowledgment. The support of this research by the Korea Science and Engineering Foundation is gratefully acknowledged. We are indebted to Prof. Gwangseo Park of Physics Department for measurements of electrical resistivity.

References

1. M. K. Wu, J. R. Ashburn, C. J. Torng, P. H. Hor, R. L. Meng, L. Gao, Z. H. Huang, Y. Q. Wang, and C. W. Chu, *Phys. Rev. Lett.*, **58**, 908 (1987).
2. S. Hwang and H. So, *Bull. Korean Chem. Soc.*, **10**, 23 (1989).
3. Y. Laligant, G. Ferey, M. Hervieu, and B. Raveau, *Europhys. Lett.*, **4**, 1023 (1987).
4. G. Xiao, M. Z. Cieplak, A. Gavrin, F. H. Streitz, A. Bakhsai, and C. L. Chien, *Phys. Rev. Letts.*, **60**, 1446 (1988).
5. T. Kajitani, K. Kusaba, M. Kikuchi, Y. Syono, and M. Hirabayashi, *Jpn. J. App. Phys.*, **27**, L354 (1988).
6. J. Ferey, A. Le Bail, Y. Laligant, M. Hervieu, B. Raveau, A. Sulpice, and R. Tournier, *J. Solid State Chem.*, **73**, 610 (1988).
7. (a) C. Jee, D. Nichols, A. Kebede, S. Rahman, J. E. Crow, A. M. Ponte Goncalves, T. Mihalisin, G. H. Myer, I. Perez, R. E. Salomon, P. Schlottman, S. H. Bloom, M. V. Kuric, Y. S. Yao, and R. P. Guertin, *J. Superconductivity*, **1**, 63 (1988); (b) Y. Oda, H. Fujita, T. Ohmich, T. Kohara, I. Nakada, and K. Asayama, *J. Phys. Soc. Jpn.*, **57**, 1548 (1988).
8. K. Kojima, K. Ohbayashi, M. Udagawa, and T. Hihara, *Jpn. J. Appl. Phys.*, **26**, L776 (1987).
9. K. Kanoda, T. Takahashi, T. Kawagoe, T. Mizoguchi, S. Kagoshima, and M. Hasumi, *Jpn. J. Appl. Phys.*, **26**, L2018 (1987).
10. B. Bleaney, K. D. Bowers, and M. H. L. Pryce, *Proc. Roy. Soc.* (London), **A228**, 166 (1955).
11. J. Stankowski, P. K. Kahol, N. S. Dalal, and J. S. Moodera, *Phys. Rev.*, **B36**, 7126 (1987).
12 See for example, T. Takabatake, M. Ishikawa, and T. Sugano, *Jpn. J. App. Phys.*, **26**, L1859 (1987).
13. F. Mehran, S. E. Barnes, T. R. McGuire, W. J. Gallgher, R. L. Sandstron, T, R, Dinger, and D. A. Chance, *Phys.*

Rev., **B36**, 740 (1987).
14. P. C. Hammel, M. Takigawa, R. H. Heffner, Z. Fisk, and K. C. Ott, *Phys. Rev. Lett.*, **63**, 1942 (1989).
15. D. L. Cox and B. R. Tress, *Phys. Rev.*, **B41**, 11260 (1990).
16. C. H. Pennington, D. J. Durand, C. P. Slichter, J. P. Rice, E. D. Bukowski, and D. M. Ginsberg, *Phys. Rev.*, **B39**, 274 (1989).
17 C. H. Pennington, D. J. Durand, C. P. Slichter, J. P. Rice, E. D. Bukowski, and D. M. Ginsberg, *Phys. Rev.*, **B39**, 2902 (1989).
18. T. Penney, M. W. Shafer, and B. L. Olson, *Int. J. Mod. Phys.*, **B1**, 1235 (1988) and references therein.
19. F. Mehran and P. W. Anderson, *Solid State Comm.*, **71**, 29 (1989).
20. D. C. Johnston *et al. Phys. Rev.*, **B36**, 4007 (1987).
21. H. Hasegawa, *Prog. Theo. Phys.*, **21**, 483 (1959).
22. K. Sugawara, *Phys. Stat. Solid.*, **B84**, 709 (1977).
23. L. Hulthen, *Ark. Mat. Astron. Fys.*, **A26**, 1 (1938).
24. P. W. Anderson, *Mater. Res. Bull.*, **8**, 153 (1973).
25. S. B. Oseroff, D. C. Vier, J. F. Smyth, C. T. Saling, S. Schultz, Y. Dalichaouch, B. W. Lee, M. B. Maple, Z. Fisk, J. D. Thompson, J. L. Smith, and E. Zimgiebl, *Solid State Chem.*, **64**, 241 (1987).
26. F. Bridges, J. B. Boyce, T. Claeson, T. H. Geballe, and J. M. Tarascon, *Phys. Rev.*, **B42**, 2137 (1990).
27. J. M. Tarascon, E. Wang, S. Kivelson, B. G. Bagley, G. W. Hull, and R. Ramesh, *Phys. Rev.*, **B42**, 218 (1990).
28. The distance between two Cu^{2+} ions separated by an O-Pd-O group is about 7.76 Å, and the maximum dipolar splitting is estimated to be 11 mT. When there are three Cu^{2+} ions in a row separated from each other by O-Pd-O groups, each line will be split into three lines. Therefore, these configurations and others will broaden the EPR spectrum. See H. So, G. P. Haight Jr., and R. L. Belford, *J. Phys. Chem.*, **84**, 1849 (1980).
29. M. Maeda, Y. Tanaka, M. Fukutomi, and T. Asaro, *Jpn. J. Appl. Phys.*, **27**, L209 (1988).
30. Z. Z. Sheng and A. M. Hermann, *Nature* (London), **332**, 420 (1988).

Study on the Biosynthesis on Neomycin: Characterization of Isocitrate Dehydrogenase of the Neomycin Producer, *Streptomyces fradiae* and its Possible Relation to the Regulation of Biosynthesis of Neomycin

Chang Hoon Lee, Yang Mo Goo*, and Kong Hwan Kim†

Department of Pharmacy, Seoul National University, Seoul 151-742
†Department of Biotechnology, Ajou University, Suwon 440-749. *Received April 18, 1991*

S. fradiae showed very high activity of isocitrate dehydrogenase compared to other microorganisms. The activity of this enzyme was increased with the growth of the organism. But the increase might not imply its involvement in the growth. Rather its increased activity seemed to have a connection with the biosynthesis of neomycin. The enzyme showed high specificity toward $NADP^+$ and D-isocitrate with Km values of 5.75 and 6.74 μM, respectively. It was activated by Mn^{2-}. Its molecular weight was estimated from its gel retardation coefficient to be in the range of 61,000-63,000 daltons and its optimum pH was 8.0. The enzyme was thermally unstable.

Introduction

In many antibiotic producing *Streptomyces* sp. it has been known that when glucose is abundant in a medium, antibiotics are scarcely produced although growth of microorganisms is dominant[1]. However as glucose in the medium is consumed, growth of the organisms is terminated and the production of antibiotics is initiated. A similar regulation has also been observed in the neomycin producer[2]. Thus it is interesting to figure out how *S. fradiae* controls the biosynthesis of neomycin.

We have been assumed that not only glucose itself had a regulation role in the biosynthesis of antibiotics, but also a metabolite which may be produced from glucose during catabolism and accumulated in the cell can have a role initiating the biosynthesis of many antibiotics[2]. As the ratio of the metabolite to glucose intaken from a medium exceeds certain value, the growth of the microorganism is terminated and the production of neomycin may be initiated. When we examined the production of neomycin by culturing *S. fradiae* in a chemically defined medium supplemented with various metabolites, fumarate was found to activate the biosynthesis of neomycin[2,3]. Furthermore, the production of neomycin in the presence of fumarate was found further activated by a small amount of glucose and repressed by a large amount of glucose[2,4]. Thus it was interesting to examine the enzymes involved in the citric acid cycle, in the metabolism of glucose or in gluconeogenesis to find out which is involved in the termination of growth, or in the initiation of biosynthesis of neomycin.